

MATHEMATICAL MODELLING OF THERMAL PROCESSES IN FRICTION STIR WELDING OF LIGHT ALLOYS BASED ON MAGNESIUM

O.O. Makhnenko, O.S. Kostenevych, O.V. Makhnenko

E.O. Paton Electric Welding Institute of the NASU
11 Kazymyr Malevych Str., 03150, Kyiv, Ukraine

ABSTRACT

Mathematical modelling of thermal processes in welding is one of the effective methods for predicting the quality of a welded joint depending on technological parameters. However, to develop an adequate mathematical model, it is necessary to take into account a number of factors that can significantly affect the accuracy of the results of the computational analysis. Using the example of the problem of mathematical modelling of temperature distributions in friction stir welding (FSW) of a butt joint of plates of magnesium MA2-1 (AZ31) alloy of different thicknesses (2 and 8 mm), a computational study of the distribution of maximum temperatures and thermal cycles at points at different distances from the welded joint axis was carried out. It was found that the results of mathematical modelling of heat conductivity processes during welding heating in FSW are influenced by several aspects. One of the significant among them is heat dissipation into the working tool and fixing tools. Also, to ensure the accuracy of calculation of temperature distributions during FSW, it is important to choose the optimal sizes of the butt joint model in order to avoid the effect of heat accumulation in a model of a limited size, and to take into account the dependence of the friction coefficient on the temperature of the material, since its value determines the power of heat generation in FSW. Based on the results obtained, recommendations are formulated for conducting mathematical modelling of thermal processes in FSW of light alloys.

KEYWORDS: friction stir welding, temperature distributions, thermal cycles, heat dissipation, work tool, backing plate, mathematical modelling, finite element analysis

INTRODUCTION

Today, mathematical modelling of various physical processes is becoming a powerful tool in the development of new technologies for the manufacture and treatment of materials, including welding and related technologies. The procedure for mathematical modelling of temperature distributions, mechanical properties, and the stress-strain state of welded joints is regulated by the acting ISO standard [1], which formulates in sufficient detail the requirements for the preparation of input data, model development, model verification and validation, calculations, analysis, and presentation of modelling results. Although the acting standard concerns computer modelling of arc welding processes, the requirements formulated there can be effectively used for other welding processes, such as friction stir welding (FSW).

The adequacy of the mathematical finite element model and the accuracy of the results obtained from the analysis of thermal processes (temperature distributions) during FSW of magnesium alloy plates depend not only on the heating source model and the choice of finite element mesh size, but also on a number of other factors, such as: taking into account heat dissipation into the working tool and fixing tools (clamps, backing plate), the overall sizes of a welded joint specimen model, variations in the

thermophysical properties of the base material, etc. It is clear that these factors can significantly affect the reliability of the results obtained from the finite element analysis, but determining the extent of their impact on the accuracy of the results of temperature distributions and thermal cycles during FSW is usually beyond the scope of the results presented in the articles or is not carried out at all. Taking into account heat dissipation into the working tool and fixing tools in the finite element model of a welded joint during FSW is found in a limited number of works [2–4]. Researchers mostly use a simplified heating source model without modelling the working tool or do not take into account heat dissipation into the fixing elements [3–6].

WITH THE AIM

of studying the impact of the above factors on the nature and magnitude of the distribution of maximum temperatures during FSW of light alloys, as well as on the parameters of thermal cycles in points at different distances from the welded joint axis, a computational study was carried out using the example of a mathematical modelling problem for temperature distributions during FSW of a butt joint of MA2-1 (AZ31) magnesium alloy plates of different thicknesses (2 and 8 mm) using FSW. Based on the results obtained, recommendations were formulated for math-

emational modelling of thermal processes during FSW of light alloys.

MATHEMATICAL MODEL OF TEMPERATURE PROCESSES DURING FSW

For mathematical modelling of residual stresses during FSW of aluminium alloy, a previously developed model [7] was used, which was supplemented by taking into account heat dissipation into the working tool and backing plate.

Heat conductivity equation in the presence of bulk heat dissipation with a power of $W(x, y, z, t)$, W/m^3 :

$$\begin{aligned} c\rho \frac{\partial T}{\partial t} = & \frac{\partial}{\partial x} \left(\lambda \frac{\partial T}{\partial x} \right) + \frac{\partial}{\partial y} \left(\lambda \frac{\partial T}{\partial y} \right) + \\ & + \frac{\partial}{\partial z} \left(\lambda \frac{\partial T}{\partial z} \right) + W(x, y, z, t), \end{aligned} \quad (1)$$

where T is the temperature, $^{\circ}C$; c is the specific heat capacity, $J/kg \cdot ^{\circ}C$; ρ is the material density, kg/m^3 ; λ is the thermal conductivity coefficient, $W/(m \cdot ^{\circ}C)$.

A distinctive feature of the developed FSW heating source model is heat generation due to friction between the tool and the joint material. The tool rotates around a vertical axis at a certain angular velocity ω , rpm/s, and is pressed against the plates with an axial force P_n , Pa, which causes a heat flow into the joint material at the contact surface of the tool (Figure 1):

$$\lambda \frac{\partial T}{\partial n} = \mu \cdot P_n \cdot \omega \cdot r, \quad (2)$$

where μ is the coefficient of friction; $r = \sqrt{(x - x_0 - v_w t)^2 + (y - y_0)^2}$ is the distance of the considered contact point from the axis of rotation of the working tool ($x_0 + v_w t, y_0$); v_w is the linear velocity of the tool.

Then, the heat dissipation power Q, W , on the corresponding contact surfaces with an area S (Figure 1) is:

$$Q = \mu \cdot P_n \cdot \omega \cdot \pi \cdot \iint_S r dS, \quad (3)$$

arm ($z = \delta, R_1 < r < R_2$)

$$Q_1 = \frac{2\pi}{3} \mu \cdot P_n \cdot \omega \cdot (R_2^3 - R_1^3),$$

side surface of the pin ($\delta - h < z < \delta, r = R_1$)

$$Q_2 = 2\pi \cdot \mu \cdot P_n \cdot \omega \cdot R_1^2 \cdot h,$$

lower end surface of the pin ($z = \delta - h, 0 > r > R_1$)

$$Q_3 = \frac{2\pi}{3} \cdot \mu \cdot P_n \cdot \omega \cdot R_1^3,$$

δ is the thickness of the plates being welded, m; h is the length of the pin entering the material, m.

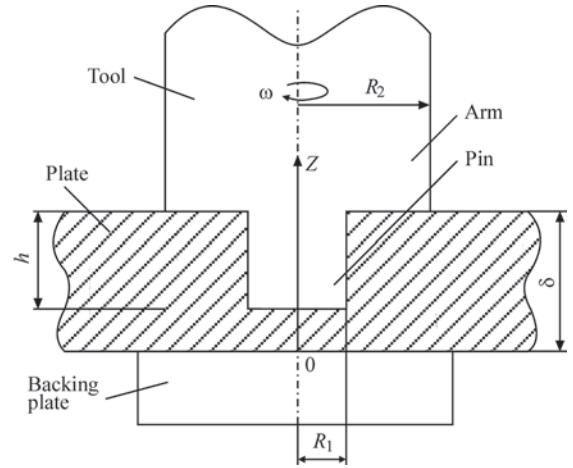


Figure 1. Schematic diagram of the working tool in FSW

In order to simplify the model, the bulk heat dissipation power $W(x, y, z, t)$, W/m^3 , can be modelled from two components. The first one is related to heat dissipation in volume V_1 on the upper surface of the joint plates under the tool arm ($\delta - dz < z < \delta, R_1 < r < R_2$); dz is the size of the finite element, and the second one is in the volume of the pin V_2 ($\delta - h < z < \delta, 0 > r > R_1$):

$$\begin{aligned} W(x, y, z, t) &= W_1 + W_2, \\ W_1 &= \frac{Q_1}{V_1} = \frac{2\pi \mu P_n \omega (R_2^3 - R_1^3)}{3 \pi (R_2^2 - R_1^2) dz} = \\ &= \frac{2\mu P_n \omega (R_2^2 + R_2 R_1 + R_1^2)}{3(R_2 + R_1) dz}, \quad (4) \\ W_2 &= \frac{Q_2 + Q_3}{V_2} = \frac{2\pi \mu P_n \omega R_1^2 h + \frac{2\pi}{3} \mu P_n \omega R_1^3}{\pi R_1^2 h} = \\ &= 2\mu P_n \omega \left(1 + \frac{R_1}{3h} \right). \end{aligned}$$

The boundary conditions on the contact surfaces between the elements of the joint and the working tool, as well as with the backing plate due to contact heat dissipation, were set in the form (Figure 2):

$$q_i = \lambda \frac{\partial T(x, y, z, t)}{\partial n} = -k_i (T_i - T), \quad (i = 1, 2) \quad (5)$$

where q_i is the heat flow at the contact surface of the tool and the welded joint ($i = 1$) and on the contact surface of the welded joint and backing plate ($i = 2$); T_i is the surface temperature of the tool or backing plate, respectively; k_i is the contact heat dissipation coefficient, $W/(m^2 \cdot ^{\circ}C)$.

The boundary conditions on the surfaces of the elements of the joint and the working tool, taking into account the convective heat exchange with the environment, were defined as follows:

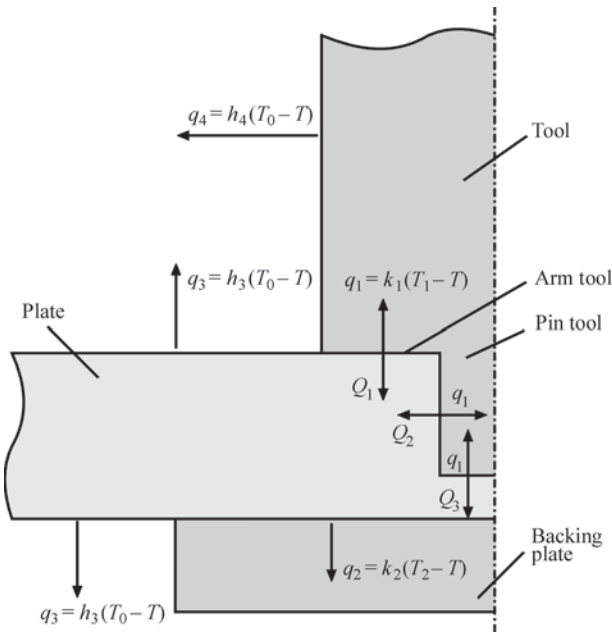


Figure 2. Schematic diagram of heat flows in FSW

$$q_i = \lambda \frac{\partial T(x, y, z, t)}{\partial n} = -h_i(T_0 - T) \quad (i = 3, 4) \quad (6)$$

where q_i is the heat flow on the surface of the welded joint elements ($i = 3$) and on the surface of the tool ($i = 4$); T_0 is the ambient temperature; h_i is the heat dissipation coefficient from the surface during convective heat exchange with the environment (usually, under conditions of natural convection in air $T_0 = 20^\circ\text{C}$, $h = 10\text{--}20\text{ W}/(\text{m}^2\cdot^\circ\text{C})$).

To perform mathematical modelling of heat dissipation processes during welding heating, data on the thermophysical properties of the base material of the joint depending on temperature are required (Table 1).

The melting temperature range [8, 9] is $T_{\text{sol}} = 605^\circ\text{C}$, $T_{\text{liq}} = 630^\circ\text{C}$, the specific heat of melting $Q_{\text{liq}} = 357\text{ kJ/kg}$. The friction coefficient for magnesium alloys is taken at a level $\mu = 0.3\text{--}0.4$ [3, 6, 9].

The material of the plate (size is $300\times 300\text{ mm}$) is MA2-1 (AZ31) magnesium alloy. The material of the FSW working tool (diameter of the arm in contact with the plate is 10 mm ; diameter in the other part of the tool is 20 mm ; total height of the tool is 50 mm) is stainless steel. The material of the

backing plate (10 mm thick and 150 mm wide) is stainless steel.

Based on the results of experimental studies [10], the technological parameters of the FSW process were set to ensure high-quality formation of a welded joint of plates with a thickness $\delta = 2$ and 8 mm . The angular velocity of the working tool was $\omega = 1420\text{ rpm}$, and the linear velocity of the tool was $v_w = 133\text{ mm/min}$.

Based on the experimental thermogram of the welding process recorded by a thermal imager, it was determined that the temperature on the outer surfaces of the welded joint plates and the tool during FSW did not exceed 355°C . According to the results of mathematical modelling, the temperature in the contact zone between the tool and the plate material will be higher (approximately at a level of $450\text{--}600^\circ\text{C}$).

For a plate with a thickness of 2 mm , the vertical pressure on the tool is $P_n = 28\text{ MPa}$. If the friction coefficient is taken as $\mu = 0.4$, then the total power of the heating source according to (4) is $W = 1.8\cdot 10^6\text{ W/m}^3$. For a plate with a thickness of 8 mm , the vertical pressure on the tool was set higher, namely $P_n = 55\text{ MPa}$. The total power of the heating source is $W = 3.5\cdot 10^6\text{ W/m}^3$ to ensure a maximum heating temperature of the material not lower than 450°C .

To account for heat dissipation in the welded joint model, it was necessary not only to create additional models of the working tool and backing plate, but also to set boundary conditions for heat dissipation and heat exchange with the environment.

The heat dissipation coefficient between the tool and the plate was taken as $k_1 = 5000\text{ W}/(\text{m}^2\cdot^\circ\text{C})$. The heat dissipation coefficient between the plate and the backing plate was assumed to be $k_2 = 1000\text{ W}/(\text{m}^2\cdot^\circ\text{C})$. The convective heat dissipation coefficient from the surface of the tool rotating at high velocity was taken as $h_1 = 50\text{ W}/(\text{m}^2\cdot^\circ\text{C})$, and the convective heat dissipation coefficient from the surface of the plate was taken as $h_2 = 20\text{ W}/(\text{m}^2\cdot^\circ\text{C})$.

The total calculation time for the FSW process is 37 s , of which the first 13 s the working tool rotates to heat the plate material to 450°C .

The procedure for selecting the size of the finite element mesh for the model for determining the temperature distribution during FSW for plates with a thickness of 2 and 8 mm was carried out, provided that when the size of the finite element is reduced twice, the relative maximum error of the results should not exceed 5% . From the data presented in Figure 4, it can be concluded that a finite element mesh size of 1 mm is optimal in terms of ensuring the necessary accuracy of results and efficient use of computer resources.

Table 1. Thermophysical properties of MA2-1 (AZ31) alloy [8]

$T, ^\circ\text{C}$	$\alpha\cdot 10^6, 1/^\circ\text{C}$	$\lambda, \text{ W}/(\text{m}\cdot^\circ\text{C})$	$c_p, \text{ J}/(\text{kg}\cdot^\circ\text{C})$	$\rho, \text{ kg}/\text{m}^3$
20	24.92	102	1008	1785
100	25.56	107	1042	1775
200	26.48	112	1076	1761
300	27.40	118	1109	1746
400	28.32	123	1143	1730
500	29.25	125	1193	1714

IMPACT OF HEAT DISSIPATION INTO THE WORKING TOOL AND FIXING TOOLS (BACKING PLATE)

Using a developed finite element model (Figures 3, 4), which contains a magnesium alloy plate, a working tool, and a stainless steel backing plate, a numerical study of the heat conductivity problem was performed during the movement of the working tool (heat source) in FSW, taking into account the heat dissipation process into the working tool and backing plate. The nature and values of the distribution of maximum temperatures during FSW of the plates were determined, as well as the parameters of thermal cycles in points at different distances from the welded joint axis (Figure 5).

Figure 6 shows the temperature distribution during FSW of 2 mm thick plates with and without account for heat dissipation into the tool and backing plate. It is seen that when heat dissipation is taken into account, the lower part of the working tool heats up quite strongly (to approximately 300 °C), and the backing plate also heats up, but noticeably less (to approximately 100 °C).

The calculation results based on thermal cycles during FSW in points at some distance from the weld axis $y = 0$; 15 and 30 mm for different variants of ac-

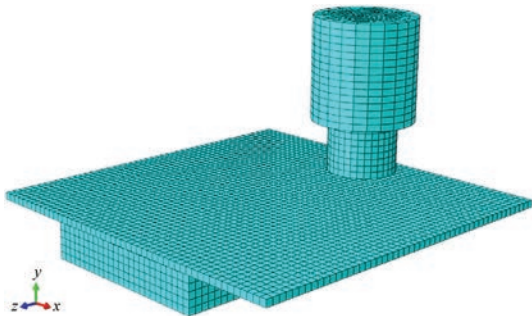


Figure 3. Finite element model of FSW, which includes a working tool, a magnesium alloy plate, and a backing plate

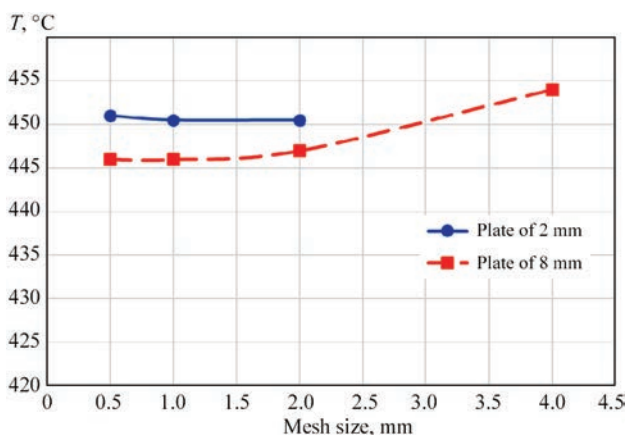


Figure 4. Dependence of the maximum values of temperature distribution in FSW on the size of the finite element mesh for plates with a thickness $\delta = 2$ and 8 mm

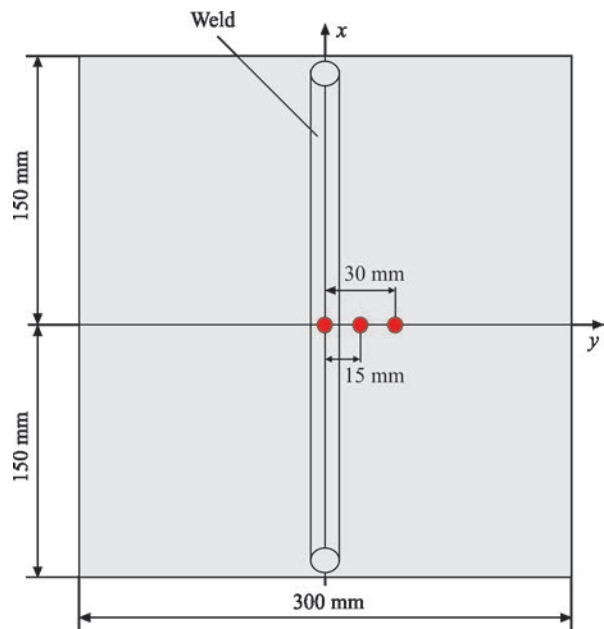


Figure 5. Layout of points on the FSW joint specimen at which thermal cycles were determined

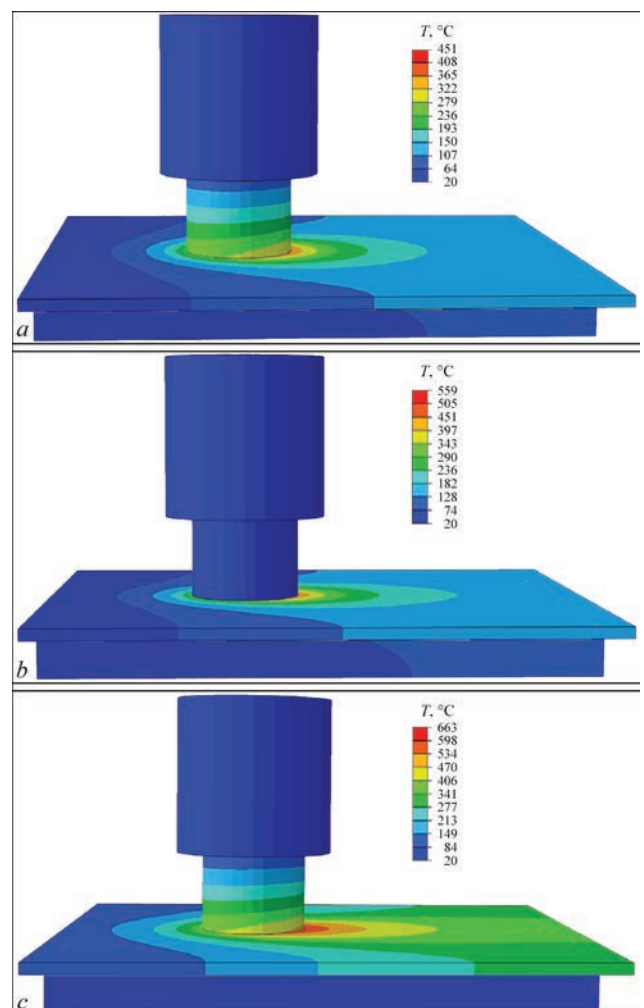


Figure 6. Temperature distribution during FSW of plates with a thickness $\delta = 2$ mm made of MA2-1 magnesium alloy: *a* — with heat dissipation into the tool and backing plate; *b* — without heat dissipation into the tool; *c* — without heat dissipation into the backing plate

Table 2. Maximum calculated temperatures during FSW of MA2-1 magnesium alloy plates depending on heat dissipation into the working tool and backing plate

Plate thickness, mm	Heat dissipation into the tool and backing plate	Without heat dissipation into the tool		Without heat dissipation into the backing plate		Without heat dissipation into the tool and backing plate	
	$T_{\max}, ^\circ\text{C}$	$T_{\max}, ^\circ\text{C}$	Relative deviation (error), %	$T_{\max}, ^\circ\text{C}$	Relative deviation (error), %	$T_{\max}, ^\circ\text{C}$	Relative deviation (error), %
2	451	559	24	663	47	890	97
8	446	498	12	512	15	540	21

count for heat dissipation showed that this factor is very important and its neglecting can lead to significant errors in the results of temperature kinetics at all stages — heating and cooling.

In the finite element analysis of the heat conductivity problem in FSW of magnesium alloy plates, neglecting of heat dissipation into the working tool and backing plate leads to significant errors (24 and 47 %, respectively) in terms of maximum temperatures for thin plates of 2 mm thick (Table 2, Figure 7, *a*).

In the case of welding thick plates of 8 mm thick, neglecting of heat dissipation into the working tool and backing plate is not so critical and is associated with errors that are 2–3 times smaller (12 and 15 %, respectively) in terms of maximum temperatures (Ta-

ble 2, Figure 7, *b*). A calculation error of 10–15 % is acceptable, considering the possible discrepancies in the input data for the calculation.

IMPACT OF THE SIZES OF THE WELDED JOINT SPECIMEN MODEL

Another very important aspect of the numerical determination of the kinetics of temperature distributions during welding is the overall sizes (width and length) of a welded joint model, since mathematical modelling requires determining the optimal model sizes to reduce calculation time while maintaining sufficient accuracy of the results.

To determine the impact of variations in the sizes of a welded joint model, a comparison was made for

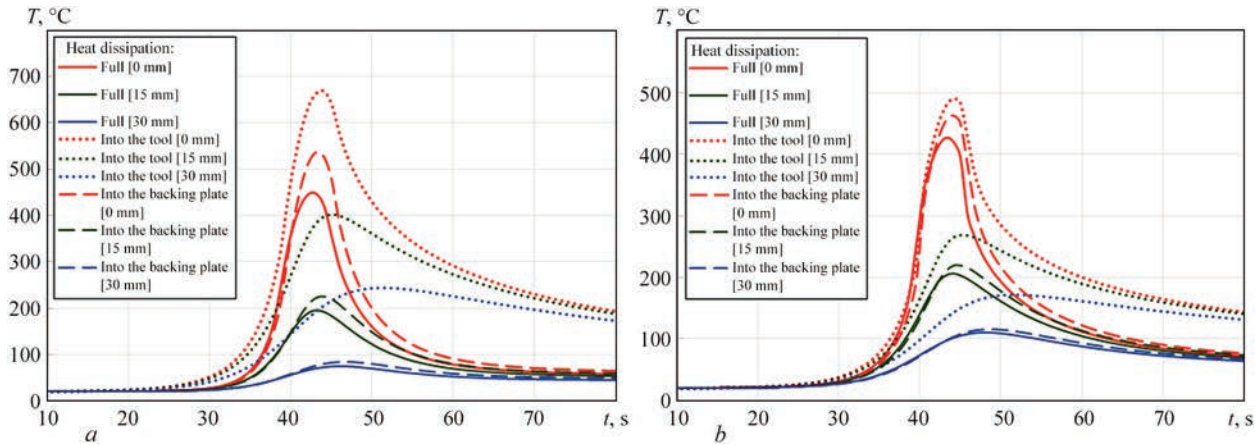


Figure 7. Effect of heat dissipation on thermal cycles during FSW in points at some distance from the weld axis $y = 0; 15$ and 30 mm (plate size 300×300 mm): *a* — thickness 2; *b* — 8 mm

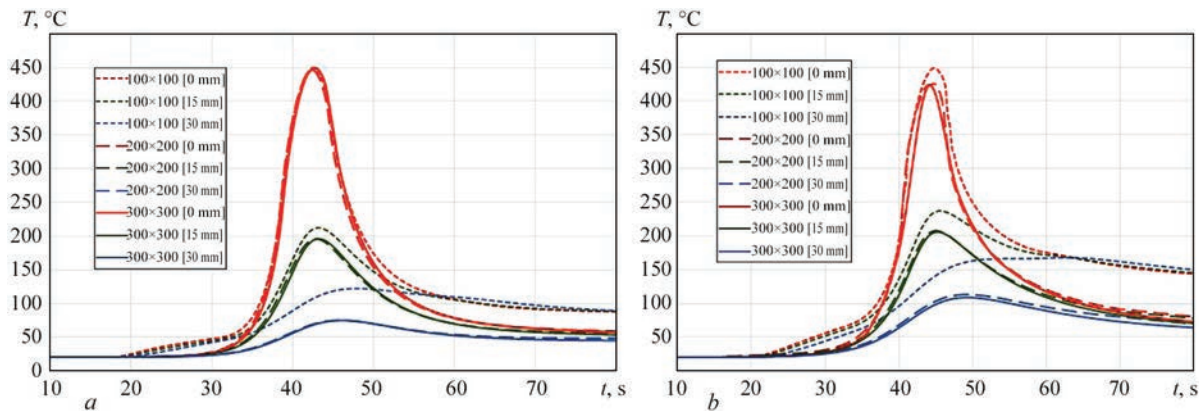


Figure 8. Thermal cycles during FSW in points at some distance from the weld axis $y = 0; 15$ and 30 mm for plates of different sizes: $100 \times 100, 200 \times 200, 300 \times 300$ mm: *a* — thickness 2; *b* — 8 mm

Table 3. Thermophysical properties of MA2-1 (AZ31) alloy [5, 8, 11]

T , °C	λ , W/(m·°C) [5]	c_p , J/(kg·°C) [5]	λ , W/(m·°C) [11]	c_p , J/(kg·°C) [11]	λ , W/(m·°C) [8]	c_p , J/(kg·°C) [8]	ρ , kg/m ³ [8]
20	96,4	1050	156	1025	102	1008	1785
100	101	1130	153	1072	107	1042	1775
200	105	1170	151	1118	112	1076	1761
300	109	1210	149	1164	118	1109	1746
400	113	1300	147	1209	123	1143	1730
500	120	1360	146	1255	125	1193	1714

the results of mathematical modelling of heat conductivity processes during welding heating in FSW for three variants of model sizes: 100×100, 200×200, and 300×300 mm. The size of the finite element mesh for all variants was maintained in accordance with the previously selected parameters.

The calculation results based on thermal cycles during FSW in points at some distance from the weld axis $y = 0$; 15 and 30 mm for plates of different sizes shown in Figure 8 indicated that at a butt joint model size of 100×100 mm, heat accumulation and, accordingly, excessive heating of the entire model occur, which leads to a significant error in the results of the thermal cycle at all its stages — heating and cooling, especially for points located at some distance from the weld axis. This effect is also enhanced for thicker plates (8 mm). The results obtained for model sizes 200×200 and 300×300 mm are very close — the error is at a level of 1–2 %. Thus, for the considered case of FSW parameters, it is possible to use a model with sizes of 200×200 mm. However, in the case of welding with higher values of heating power in FSW, as well as for arc welding, the model size of 300×300 mm is more optimal in terms of ensuring the accuracy of the temperature field results.

IMPACT OF VARIATION OF VALUES IN THE THERMOPHYSICAL PROPERTIES OF THE MATERIAL

As shown by the analysis of literature data, there is a noticeable difference in the values of these properties

(Table 3, Figure 9) with regard to data on the thermophysical properties depending on the temperature of the base material of the welded joint of AZ31 (MA2-1) magnesium alloy [5, 8, 11].

To determine the effect of variations in the values of the thermophysical properties of the material, a comparison was made for the results of mathematical modelling of heat dissipation (thermal conductivity) processes during welding heating in FSW for three variants of these properties. Two variants of properties were taken from literature sources specifically for the AZ31 (MA2-1) alloy, and the third variant corresponds to pure Mg, since this chemical element constitutes approximately 95 % of the alloy under consideration.

Figure 10 shows the results of calculating thermal cycles during FSW in points at some distance from the weld axis $y = 0$; 15 and 30 mm for a 300×300 mm plate and based on different thermophysical properties. It is seen that if the values of the properties differ within 5 %, as for the data [5, 8], then the error of the thermal cycle results does not exceed a few percent. In the case of a significant (from 20 to 50 %) deviation in the thermal conductivity coefficient of pure Mg [11], the results for the maximum temperatures of thermal cycles already have an error of more than 20 %. I.e., the variation in the values of the thermophysical properties of the material can lead to an error in the results of mathematical modelling of heat conductivity processes during welding heating in FSW,

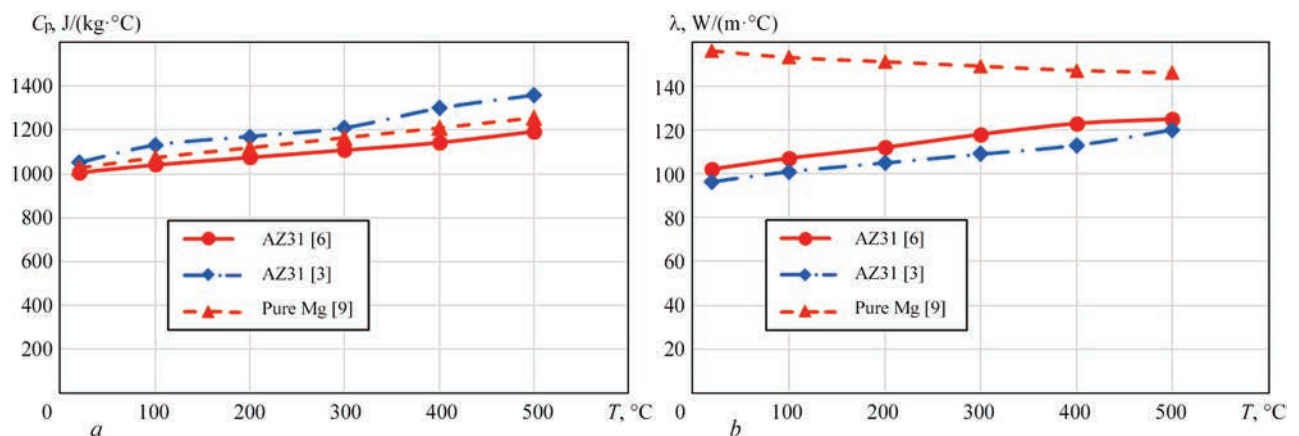


Figure 9. Dependence of the specific heat capacity and thermal conductivity of AZ31 magnesium alloy on temperature according to various data [5, 8, 11]

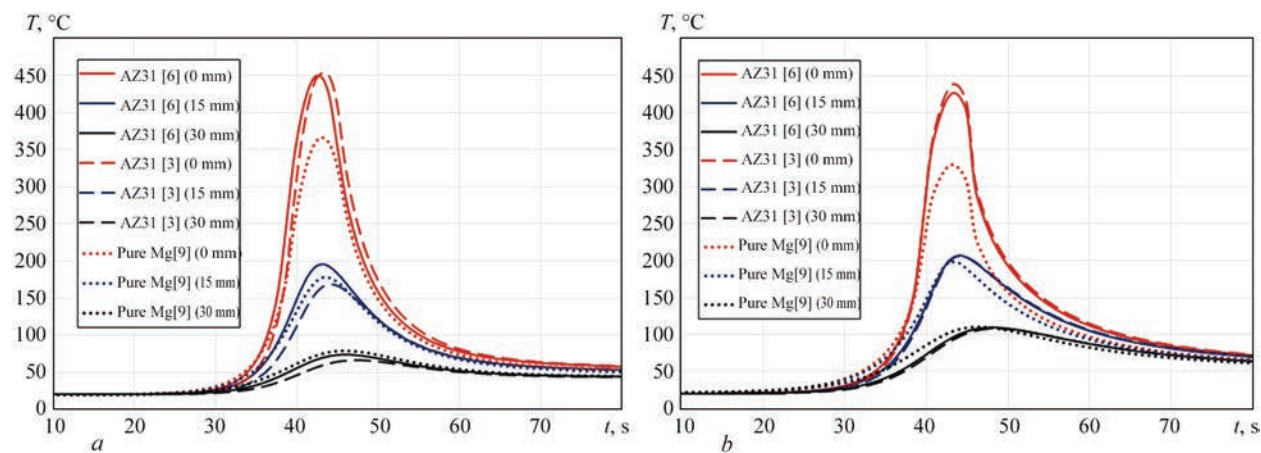


Figure 10. Thermal cycles during FSW in points at some distance from the weld axis $y = 0$; 15 and 30 mm and according to various data on thermophysical properties (300×300 mm plates): a — thickness of 2; b — 8 mm

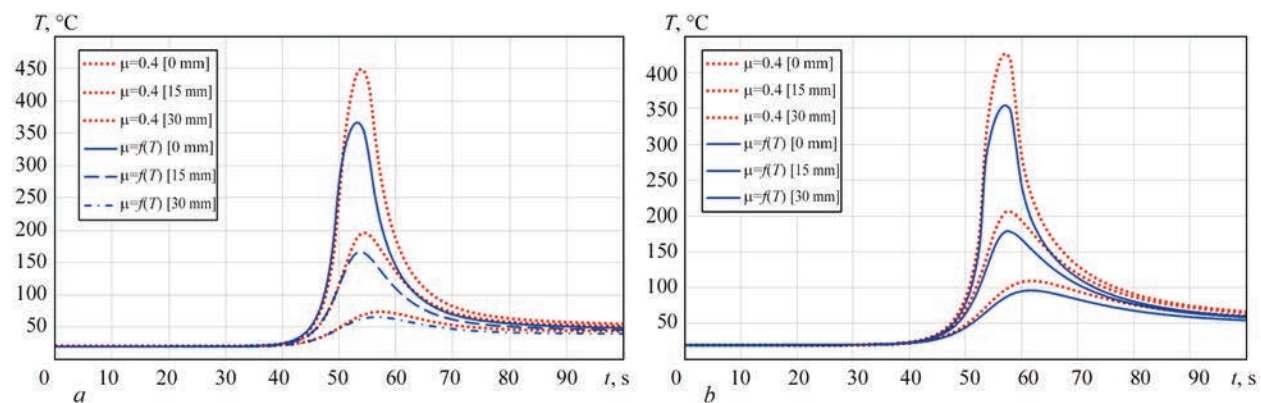


Figure 11. Thermal cycles during FSW in points at some distance from the weld axis $y = 0$; 15 and 30 mm according to various data on the dependence of friction coefficient on temperature (300×300 mm plate): a — thickness of 2; b — 8 mm

Table 4. Dependence of friction coefficient on temperature [12]

$T, ^\circ\text{C}$	μ
20	0.4
100	0.4
200	0.4
250	0.4
300	0.35
400	0.25
500	0.09

but this error corresponds to the deviation in the values of the properties themselves.

The influence of the dependence of friction coefficient on temperature on the results of modelling temperature distributions during FSW of magnesium alloy plates was also investigated. Figure 11 shows the thermal cycles during FSW of plates of 300×300 mm and with a thickness $\delta = 2$ and 8 mm in points at some distance from the weld axis $y = 0$; 15 and 30 mm according to different data on the dependence of the friction coefficient on temperature, namely at a constant value $\mu = 0.4$ and at a dependence of $\mu = f(T)$ (Table 4) [12]. According to the thermal cycles presented in Figure 11, at a constant value of the friction

coefficient, higher values of maximum temperatures were obtained.

CONCLUSIONS

1. In finite element analysis of heat conductivity problem during FSW of thin 2 mm thick magnesium alloy plates, neglecting of heat dissipation into the working tool and fixing tools leads to significant errors in the maximum temperature values (above 40 %) and for thick plates with a thickness of 8 mm, this error is no longer so critical (up to 15 %).

2. With a limited size of a butt joint model of 100×100 mm, heat accumulation and excessive heating of the entire model are observed, which leads to a significant error in the results of the thermal cycle at all its stages — heating and cooling, especially for points at some distance from the weld axis. This effect is also enhanced for thicker plates (8 mm). For the considered case of FSW parameters, it is possible to use a model with sizes of 200×200 mm to determine the temperature distributions, but in the case of welding with higher heating power values, a model size of 300×300 mm will be more optimal in terms of ensuring the accuracy of the temperature field results.

3. Variations in the values of thermophysical properties of the material can lead to errors in the results of mathematical modelling of heat conductivity processes during welding heating in FSW, but this error, as a rule, does not exceed the deviation of the properties themselves. The dependence of the friction coefficient on the material temperature is important for ensuring the accuracy of calculating temperature distributions during FSW, since its value determines heat generation power during FSW.

REFERENCES

1. ISO/TS 18166:2016: *Numerical welding simulation — Execution and documentation*.
2. Zhenzhen, Yu, Wei Zhang, Hahn Choo, Zhili Feng (2012) Transient heat and material flow modeling of friction stir processing of magnesium alloy using threaded tool. *Metallurgical and Materials Transact. A*, **43**, 724–737. DOI: <https://doi.org/10.1007/s11661-011-0862-1>
3. Song, M., Kovacevic, R. (2004) Heat transfer modelling for both workpiece and tool in the friction stir welding process: A coupled model. *Proc. Inst. Mech. Eng., Pt B: J. of Engineering Manufacture*, 218(1), 17–33. DOI: <https://doi.org/10.1243/095440504772830174>
4. Majstrenko, A.L., Nesterenkov, V.M., Dutka, V.A. et al. (2015) Modeling of heat processes for improvement of structure of metals and alloys by friction stir method. *The Paton Welding J.*, **1**, 2–10. DOI: <https://doi.org/10.15407/tpwj2015.01.01>
5. Gok, A., Aydin, M. (2013) Investigations of friction stir welding process using finite element method. *The Inter. J. of Advanced Manufacturing Technology*, **68**, 775–780. DOI: <https://doi.org/10.1007/s00170-013-4798-z>
6. Serindag, H.T., Kiral, B.G. (2017) Friction stir welding of AZ31 magnesium alloys — A numerical and experimental study. *Latin American J. of Solids and Structures*, 14(1), 113–130. DOI: <https://doi.org/10.1590/1679-78253162>
7. Tsaryk, B.R., Muzhychenko, O.F., Makhnenko, O.V. (2022) Mathematical model of determination of residual stresses and strains in friction stir welding of aluminium alloy. *The Paton Welding J.*, **9**, 33–40. DOI: <https://doi.org/10.37434/tpwj2022.09.06>
8. JMatPro® — Practical Software for Materials Properties. <https://www.sentessoftware.co.uk>
9. He Yang, Liang Huang, Mei Zhan (2011) Hot forming characteristics of magnesium alloy AZ31 and three-dimensional FE modeling and simulation of the hot splitting spinning process. In: *Magnesium alloys — Design, processing and properties*. Ed. by F. Czerwinski, 367–388. DOI: <https://doi.org/10.5772/13778>
10. Khokhlov, M.A., Makhnenko, O.O., Kostin, V.A. et al. (2024) Thermomechanical processes in friction stir welding of magnesium alloy sheets. *Avtomatychne Zvaryuvannya*, **3**, 3–10 [in Ukrainian]. DOI: <https://doi.org/10.37434/as2024.03.01>
11. Larikov, L.N., Yurchenko, Yu.F. (1985) *Structure and properties of metals and alloys: Thermal properties of metals and alloys*: Handbook. Kyiv, Naukova Dumka [in Russian].
12. Khairuddin, J. (2013) *Development of multicomponent loads, torque and temperature measurement device for friction stir welding process*. School of Mechanical Engineering University Sains Malaysia. DOI: <https://doi.org/10.13140/RG.2.1.2165.0085>

ORCID

O.O. Makhnenko: 0000-0003-2319-2976,
O.S. Kostenevych: 0000-0002-7427-2805,
O.V. Makhnenko: 0000-0002-8583-0163

CONFLICT OF INTEREST

The Authors declare no conflict of interest

CORRESPONDING AUTHOR

O.O. Makhnenko
E.O. Paton Electric Welding Institute of the NASU
11 Kazymyr Malevych Str., 03150, Kyiv, Ukraine.
E-mail: makhnenko@paton.kiev.ua

SUGGESTED CITATION

O.O. Makhnenko, O.S. Kostenevych,
O.V. Makhnenko (2025) Mathematical modelling
of thermal processes in friction stir welding of light
alloys based on magnesium. *The Paton Welding J.*,
9, 10–17.
DOI: <https://doi.org/10.37434/tpwj2025.09.02>

JOURNAL HOME PAGE

<https://patonpublishinghouse.com/eng/journals/tpwj>

Received: 08.04.2025

Received in revised form: 30.06.2025

Accepted: 15.09.2025

THE FUTURE OF THE WELDING AND CUTTING INDUSTRY

The Ultimate World of Cutting and Welding — Urban Steel Expo

With The Ultimate World of Cutting and Welding — Urban Steel Expo (USE), Messe Düsseldorf has developed a novel concept specifically tailored to the needs of the welding and cutting industry. This groundbreaking platform combines technology, business, and event culture, enabling a new form of exchange and networking.

Debut in April 2027 — a new chapter for the industry

USE will debut from **20 to 23 April 2027**, turning Düsseldorf Exhibition Centre into the international hub for companies from the sectors of welding, cutting and related processes and technologies every four years. The launch of USE 2027 will re-define classical trade fairs. Technology, business, creativity, and community merge into an industry event. The new format brings together global market and innovation leaders, showcasing groundbreaking technologies.